



Corrosion Inhibition Behavior of DL-Methionine and L-Tryptophan on Carbon Steel

Achmad Rochliadi ^{1,*}, Aep Patah ¹, Claudia ¹, Dadang Ramadhan ¹

¹ Research Division of Inorganic and Physical Chemistry, Faculty of Mathematics and Natural Sciences, Institut Teknologi Bandung, Bandung, Indonesia

* Corresponding author: achmad@itb.ac.id

<https://doi.org/10.14710/jksa.26.7.249-260>



Article Info

Article history:

Received: 11th May 2023
 Revised: 06th October 2023
 Accepted: 09th October 2023
 Online: 05th November 2023

Keywords:

Corrosion; bio-inhibitors;
 Amino Acids; DL-Methionine;
 L-Tryptophan

Abstract

The cost-effective, efficient, and environmentally friendly corrosion inhibitors have become increasingly significant within the oil and gas sector. Consequently, this research was conducted to evaluate the corrosion inhibition behavior of the amino acids DL-Met and L-Tryp on carbon steel in acidic (0.05 M HCl), alkaline (0.05 M NH₄OH), and neutral (3% NaCl) environments. This study used Electrochemical Impedance Spectroscopy (EIS) and Potentiodynamic Polarization (PDP) to assess the performance of amino acids as corrosion inhibitors. The EIS and PDP measurements revealed that DL-Met and L-Tryp exhibited corrosion inhibition effects exclusively in acidic conditions. In this environment, DL-Met demonstrated a corrosion inhibition efficiency (η) of 49.7% at a concentration of 525 ppm, while L-Tryp reached an efficiency of 87.08% at a concentration of 25 ppm. Under the same conditions, DL-Met reduced the corrosion rate from 10 mm/year to 4.468 mm/year, and L-Tryp reduced it from 10.95 mm/year to 5.003 mm/year. However, the corrosion inhibition activity of DL-Met and L-Tryp in neutral and alkaline conditions did not yield positive results according to EIS measurements. In neutral conditions, 100 ppm DL-Met exhibited -22.46% inhibitory activity. Meanwhile, in alkaline conditions, 150 ppm DL-Met and 5 ppm L-Tryp exhibited inhibition efficiencies of -72.39% and -81.9%, respectively. This research aims to provide the oil and gas industry with a natural-based corrosion inhibitor alternative, offering a solution to corrosion-related challenges in acidic conditions.

1. Introduction

In industries related to chemical transportation and storage, especially in sectors such as oil and gas, corrosion poses a significant and inherent challenge, necessitating effective mitigation strategies due to its potential for adverse economic repercussions [1, 2]. Corrosion occurs when metals deteriorate due to concurrent electrochemical reactions involving oxidation and reduction processes [3]. When steel comes into contact with a corrosive environment, the iron it contains undergoes oxidation, leading to the formation of iron oxide, commonly known as rust. At the same time, other elements in the corrosive environment, like water vapor and oxygen, undergo reduction reactions. Prolonged oxidation of steel can lead to structural damage [4].

In the United States, an annual budget of over 1 trillion dollars is allocated to address steel corrosion issues across various industrial sectors [5]. To address this challenge, various corrosion inhibitors, including chromate, phosphate, and benzotriazole, have been developed. These materials are used to combat corrosion [6, 7]. Nonetheless, the improper application and mishandling of these traditional inhibitors can lead to environmental contamination and pose safety risks to workers due to the presence of carcinogenic properties in some of their components.

To mitigate the potential hazards associated with conventional corrosion inhibitors, biomaterial-based inhibitors have been developed, such as plant extracts, seeds, fruit peels, and other materials like amino acids [8]. These materials are considered more cost-effective,

safe, and eco-friendly when compared to conventional inhibitors [9]. Some biomaterial extracts possess unique structures and active groups that enable them to be adsorbed both physically and chemically onto the metal surface. The active groups facilitating this adsorption process include heteroatoms (N, S, P) and unsaturated benzene rings [10, 11, 12]. When bio-inhibitor materials adsorb onto the metal surface, the electron transfer process between the metal surface and the corrosive environment becomes impeded, directly inhibiting the corrosion process [13]. Some bio-inhibitors are equipped with carbon chain structures, providing hydrophobic properties that protect the metal surface from the corrosive environment [14].

Table 1 presents several previous studies investigating the inhibitory activity of bio-inhibitors. Based on previous research on bio-inhibitors, they can serve as an alternative to conventional corrosion inhibitors. Most researchers choose acidic conditions as the electrochemical measurement medium to determine the inhibitory activity of bio-inhibitors. This is due to the corrosion problem in the petroleum industry caused by environments with a pH below 5 [15]. Corrosion, however, is not limited to acidic conditions; it can also occur in high-ion environments or under conditions with a pH above 10 [16]. Evaluating the performance of bio-inhibitors under various conditions (acidic, alkaline, and neutral with high electrolytes) is necessary to draw

comprehensive conclusions that can be applied in the petroleum industry.

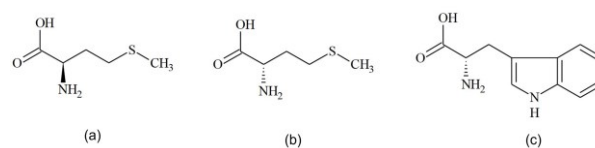


Figure 1. Structures of (a) D-methionine, (b) L-methionine, and (c) L-tryptophan

This research investigates the corrosion inhibition behavior of materials derived from the amino acids DL-Met and L-Tryp on carbon steel surfaces under acidic conditions (pH < 5), high electrolyte conditions (neutral pH), and alkaline conditions (pH > 10). Methionine and tryptophan are water-insoluble, non-toxic, and easy to produce. Their ability to adhere to metal surfaces makes them potential corrosion bio-inhibitor candidates [17]. The isoelectronic structures of DL-Met and L-Tryp are shown in Figure 1. The amino acids DL-Met and L-Tryp both contain heteroatoms (S, N, and O) in their structures. Tryptophan also has a benzene ring, providing a lone pair of electrons that facilitates adsorption via an electron transfer mechanism [18]. Preventing corrosion in carbon steel materials is crucial, and there is a significant demand for safe and cost-effective inhibitors. DL-Met and L-Tryp have shown promising potential as inhibitors due to their unique chemical structures.

Table 1. The list of previous studies investigating bio-inhibitors

No	Bio-inhibitors	Metals/Alloys	Condition	η (%) /concentration Inhibitors	Ref.
1	<i>Sonchus arvensis</i> weed extract	Mild Steel	Acid (0.5 M HCl)	97/500 ppm	[8]
2	Amino acids: L-asparagine (L-Asp), L-proline (L-Pro), and Lisoleucine (L-Iso)	Mild Steel	Acid (0.5 M HCl)	91 to 95/1000 ppm	[19]
3	Amino acids: L-alanine (L-Ala), and L-leucine (L-Leu)	Cu	Computational Calculation	-	[20]
4	Amino acid derivatives: 2-phenylthiazolidine-4-carboxylic acid and 2-(thiophene-2-yl) thiazolidine-4-carboxylic acid	Carbon Steel	Acid condition (pH 5.4)	99.1 to 99.3/08 mM	[21]
5	Extract of <i>Cnicus benedictus</i> weed	Mild Steel	Acid (0.5 M HCl)	92.45/1000 ppm	[22]
6	Extract of <i>Hymenaea stigonocarpa</i> fruit shell	Steel	Acid (0.5 M H ₂ SO ₄)	87.2/1233.4 ppm	[23]
7	<i>Andrographis echiodides</i> leaves extract	Mild Steel	Acid (1 M HCl)	79.48/1% (v/v)	[24]
8	<i>Gloriosa superba</i> seeds extract	Carbon Steel	Acid (0.5 M H ₂ SO ₄)	93.84/700 ppm	[25]
9	amino acids L-histidine and L-cysteine	Carbon Steel	the oilfield formation water	98/0.4 mM	[26]
10	L-Tryptophan	Carbon Steel	Acid (1 M HCl)	90.8/10 mM	[27]

Previous research has investigated the inhibitory activity of DL-Met and L-Tryp. Fu *et al.* [27] conducted L-Tryp inhibition experiments using an optimal concentration of 10 mM in a 1 M HCl solution. Luo *et al.* [28] reported L-Tryp inhibition with an optimal concentration of 200 ppm in the same solution. Meanwhile, under neutral conditions with 3% NaCl, Wint *et al.* [29] observed that L-Tryp did not exhibit an inhibitory effect but resulted in corrosion inefficiency. Furthermore, there is limited research on the inhibitory activity of pure L-Tryp in alkaline conditions. On the other hand, Zhang *et al.* [30] investigated the corrosion inhibition activity of DL-Met with an optimum concentration of 0.01 M under acidic conditions of 0.5 M HCl. In addition, Kiliççeker and Demir [31] reported the inhibitory activity of DL-Met on copper metal in 3.5% NaCl with an optimum inhibitor concentration of 0.01 M. However, not many researchers have reported the inhibitory activity of DL-Met in alkaline conditions.

Therefore, this research aims to conduct a follow-up study on the corrosion inhibition activity using lower concentrations of DL-Met and L-Tryp bio-inhibitors (in ppm units) compared to previous studies. This work also examines the corrosive environmental conditions that resemble those in the oil, gas, and mining industries, including acidic conditions (0.05 M HCl), neutral conditions (3% NaCl) specific to DL-Met, and basic conditions (0.05 M NH₄OH) [15, 16]. The inhibitory effects were assessed using electrochemical techniques, such as Electrochemical Impedance Spectroscopy (EIS) and Potentiodynamic Polarization (PDP). This study offers valuable insights for future research in developing bio-inhibitors and expanding their applications in various industrial sectors.

2. Experimental

DL-Methionine (DL-Met) and L-Tryptophan (L-Tryp) were assessed for their inhibitory properties using two electrochemical techniques: Electrochemical Impedance Spectroscopy (EIS) and Potentiodynamic Polarization (PDP). This section outlined the research methodology, including the materials and equipment used, the preparation of electrodes and inhibitors, the preparation of the medium, and the process of conducting EIS and PDP measurements.

2.1. Materials

The materials used in this study included 1 × 1 cm carbon steel strips, tin solder, resin, and hardener for preparing the working electrodes. The electrolyte solution was prepared by dissolving 3 g of solid NaCl, 1.519 mL of 10% HCl solution, and 0.779 mL of 25% NH₄OH solution in 100 mL of water. The choice of media aimed to replicate corrosive environments in the oil and gas industries. For instance, 0.05 M HCl (pH ≈ 2) was selected to simulate the acidic conditions in the petroleum industry [15, 16]. Additionally, 0.05 M NH₄OH (pH ≈ 12) was chosen to replicate the environment in the gas sector, particularly in ammonia gas production [32], and 3% NaCl (pH = 7) to simulate the corrosive conditions in offshore oil drilling [33]. Electrode cleaning was performed using technical-grade ethanol. The saturated

KCl solution was used to soak the saturated calomel electrode (SCE), while the 0.01 M KCl solution was used as the salt bridge for the three electrodes. The inhibitor solution was prepared by dissolving solid DL-methionine (Merck Sigma-Aldrich, 99%) and L-Tryptophan (Merck Sigma-Aldrich, 99%) in water.

2.2. Equipment

The preparation of electrodes and electrolyte solutions required standard laboratory glassware, copper wire, pliers, solder, ice molds, 600 and 1000 silicon carbide (SiC) paper, an analytical balance, a spatula, and a multimeter. The EIS method for assessing electrochemical parameters employed an electrochemical cell, a platinum electrode, a saturated calomel electrode (SCE), and the Gamry Ref3000 device (Potentiostat/Galvanostat/ZRA). Meanwhile, the PDP method for determining the electrochemical parameters involved using the VoltaLab device (VoltaLab PGZ 301) and Voltmaster 4 software.

2.3. Electrode Preparation

To prepare the carbon steel electrodes, 1 cm × 1 cm carbon steel strips were soldered to one end of a wire and placed on an ice mold. Once solidified, a blend of a 3:2 ratio of resin and hardener was poured into the mold to cover the steel surface. After leaving the mixture to harden for a day, the steel electrode candidates were removed from the mold. The working electrode underwent a polishing process using progressively finer grits of silicon carbide (SiC) paper until it had a smooth and shiny surface. Subsequently, the electrode was cleansed with ethanol and allowed to dry.

2.4. Inhibitor Preparation

Solid DL-Met (0.25 g) was weighed and dissolved in 250 mL of deionized water. Solid L-Tryp (0.01 g) was weighed and dissolved in 100 mL of deionized water.

2.5. Medium Preparation

To prepare the medium solution in an acidic environment, 1.519 mL of 10% HCl stock solution was used to create a 0.05 M HCl solution with a pH of 1.3. Similarly, a medium solution under alkaline conditions, specifically 0.05 M NH₄OH (pH = 12.7), was prepared by dissolving 0.779 mL of 25% NH₄OH stock solution in deionized water until the final volume reached 100 mL for each solution. While preparing the solutions for use, consistency in their properties could be guaranteed, as they were sourced from the same batch, thus ensuring uniformity in all measurements. However, the conditions of the working electrode may vary; for example, after initial use, the electrode's state may deviate from its initial condition. Additionally, when creating two electrodes, there is a possibility that the dimensions of one electrode may differ from the other.

2.6. EIS and PDP Measurements

The electrochemical cell system consisted of a three-electrode system, with the working electrode made of steel, a counter electrode made of platinum (Pt), and a reference electrode made of a saturated calomel electrode

(SCE). This system was immersed in a medium of 3% (w/v) NaCl for neutral conditions, 0.05 M HCl for acidic conditions, and 0.05 M NH₄OH for alkaline conditions. The system was then connected to a computer using a Gamry Ref3000 device (Potentiostat/Galvanostat/ZRA). The Potentiostatic EIS was selected in the Gamry Framework software with a frequency range of 10⁴ Hz to 10⁻¹ Hz as the measurement condition.

The open-circuit potential (OCP) measurement took about 15 minutes. Attaining an OCP value within ±2 mV after 10 minutes indicated a sufficiently stable electrochemical condition [34]. All experiments were carried out at room temperature. The PDP measurements were conducted using a three-electrode system immersed in the same medium as the EIS method. The system was connected to a computer via the VoltaLab device (VoltaLab PGZ 301) and Voltmaster 4 software, configured to perform corrosion measurements, including OCP and Tafel extrapolation.

3. Results and Discussion

3.1. EIS Data Interpretation and Processing

EIS measurements were conducted on carbon steel at various pH levels and inhibitor concentrations, resulting in Nyquist plots and equivalent circuits. Electrochemical parameters such as solution resistance (R_s), electric double-layer capacitance (C_{dl}), charge transfer resistance (R_{ct}), constant phase element (CPE), and Warburg resistance (W) were determined using an equivalent circuit. R_s is associated with the kinetics of ions in an electrolyte solution, while R_{ct} describes the electron transfer process at the electrode surface [10]. The dominant corrosion process on the working electrode can be identified by analyzing the equivalent circuit. The R parameters and R_{ct} were utilized to assess the inhibitory activity's efficiency by plotting them against inhibitor concentrations. Furthermore, the R parameter of the equivalent circuit can be used to calculate the percentage inhibition efficiency (η) using Equation (1) [6].

$$\eta = \left(1 - \frac{R_{blank}}{R_{inhibitor}}\right) \times 100\% \quad (1)$$

The processing of EIS data helped the determination of the optimal conditions for DL-Met and L-Tryp to exhibit inhibitory activity. After establishing these optimal conditions, further investigations were conducted using the Potentiodynamic Polarization (PDP) method.

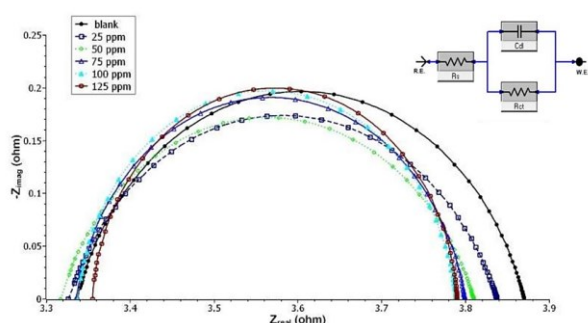


Figure 2. Nyquist plot of carbon steel with DL-Met inhibitor in 3% NaCl

EIS measurements were initially conducted to evaluate the inhibitory activity of DL-Met on steel in a 3% NaCl solution (pH neutral). Figure 2 depicts the Nyquist plot of carbon steel in 3% NaCl with the DL-Met inhibitor. The shape of the Nyquist plot suggests a simple Randles circuit with the parameters C_{dl}, R_s, and R_{ct}. The R_{ct} concentration plot is shown in Figure 3a, while Figure 3b displays the R_s concentration plots. R_{ct} and R_s exhibited a relatively decreasing trend with DL-methionine added at neutral pH.

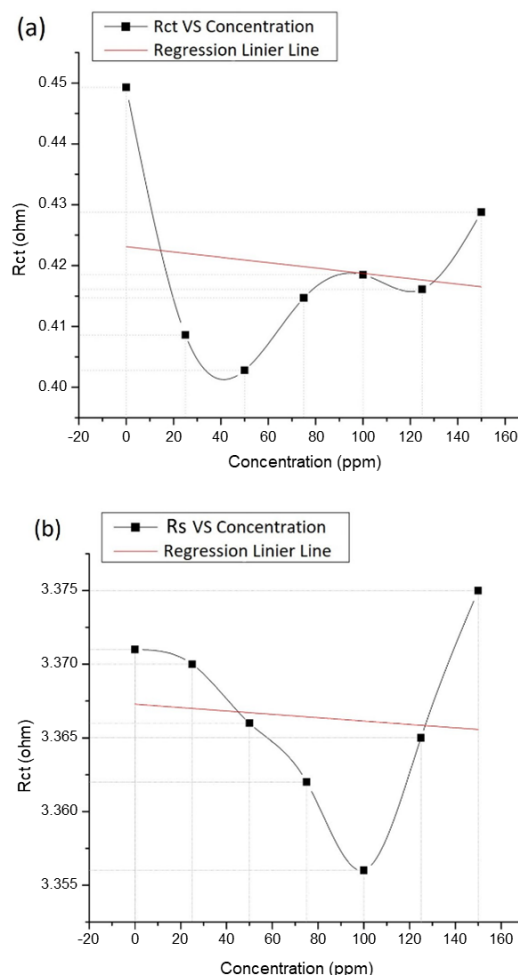


Figure 3. (a) Plot of DL-Met concentration against R_{ct} in 3% NaCl, and (b) Plot of DL-Met Concentration against R_s in 3% NaCl

Table 2. Parameter data for equivalent circuit components of carbon steel with DL-Met inhibitor in 3% NaCl solution

[DL-Met] (ppm)	R _{ct} (Ω cm ²)	R _s (Ω cm ²)	C _{dl} (mF)	η R _{ct} (%)	η R _s (%)	η _{total} (%)
Blank	0.500	3.387	0.481	-	-	-
25	0.445	3.390	0.392	-12.250	0.080	-12.170
50	0.421	3.383	0.206	-18.830	-0.110	-18.940
75	0.422	2.361	0.127	-18.550	-43.450	-62.000
100	0.412	3.350	0.112	-21.360	-1.100	-22.460

Therefore, when Equation 1 is applied to calculate the percentage efficiency, it yields a negative η value, as shown in Table 2. Table 2 presents the parameters and η values from the EIS measurements for different DL-Met concentrations in the 3% NaCl solution. Thus, it can be inferred that DL-methionine is not a suitable inhibitor under neutral pH conditions but acts as a catalyst in the corrosion reaction at low concentrations of DL-Met (ppm units).

In contrast to Kiliñçeker and Demir [31], which used a much higher concentration of DL-Met (Molar units), which provided an inhibitory effect. Thus, it can be concluded that DL-Met cannot be deposited on metal surfaces at low concentrations (ppm units). Instead, it only dissolves in solution, which ultimately facilitates the corrosion process by accelerating the rate of oxidation-reduction reactions. This is corroborated by information about the solubility properties of amino acids, which easily dissolve in neutral and alkaline pH conditions [35]. Under neutral and alkaline pH levels, DL-Methionine and L-Tryptophan will convert into zwitterions [36], enhancing solution conductivity and resulting in a negative R_s value in this measurement, indicating no inhibitory activity. The effect of pH on the structure of amino acids was discussed in another section of this paper.

Furthermore, EIS measurements were conducted to investigate the inhibitory activity of DL-Met on carbon steel electrodes in 0.05 M HCl solution. Figure 4 displays the Nyquist plot for the carbon steel electrode in 0.05 M HCl with the addition of a DL-Met inhibitor. After obtaining the Nyquist plot, circuit matching was performed to obtain the Randles equivalent circuit with Warburg. In an acidic environment, the working electrode's surface can develop a metal oxide film, introducing the constant phase element (CPE) parameter. This metal oxide film contains pores that facilitate ion transfer processes, resulting in the appearance of the Warburg (W) parameter [37].

Concentration plots were generated for R_{ct} and R_s against the DL-Met concentration to investigate the inhibitory activity trend. Figures 5a and 5b illustrate the relationship between DL-Met concentration and R_{ct} or R_s values in 0.05 M HCl. The data clearly indicate an increase in both R_{ct} and R_s values as the DL-Met concentration increases, implying a higher degree of inhibitory activity for carbon steel in 0.05 M HCl. The equivalent circuit component parameter data for carbon steel in 0.05 M HCl with DL-Met inhibitor are presented in Table 3.

In this measurement, the highest inhibition efficiency of DL-Met in 0.05 M HCl solution was achieved when 525 ppm DL-Met was added with a total efficiency value of 49.7%. Thus far, it can be concluded that DL-Met can provide inhibitory activity at $\text{pH} < 7$ (acidic conditions), with the greatest inhibition efficiency at a concentration of 525 ppm. The inhibition activity of adding 525 ppm DL-Met in 0.05 M HCl is the optimum condition, which was investigated further using the PDP method.

Then, EIS measurements were carried out to determine the inhibitory activity of L-Tryp on carbon steel in 0.05 M HCl under acidic conditions. Figure 6 displays the Nyquist plot of the L-Tryp activity measurements in 0.05 M HCl, the same as the EIS measurement before (DL-Met under acidic conditions).

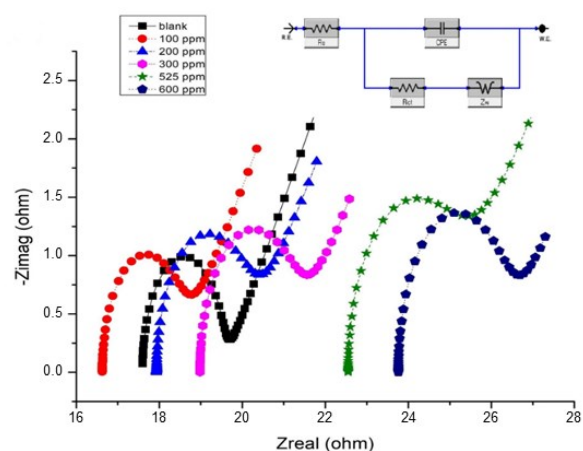


Figure 4. Nyquist plot for carbon steel with DL-Met inhibitor in 0.05 M HCl solution

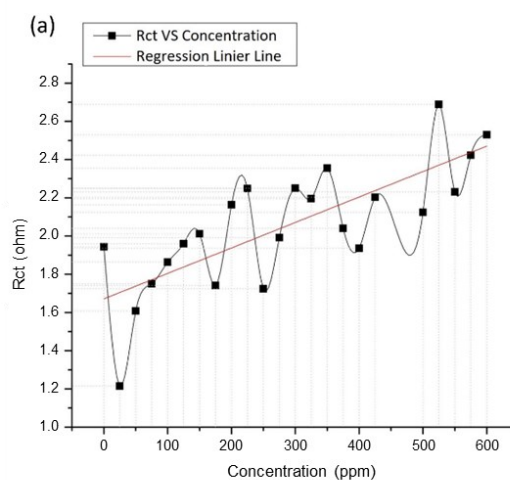
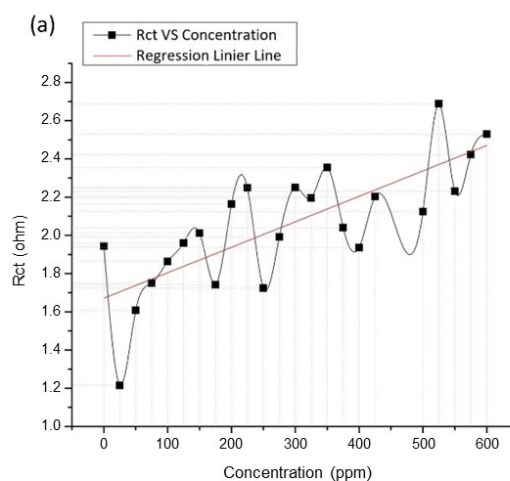


Figure 5. (a) The plot of DL-Met Concentration against R_{ct} in 0.05 M HCl solution, and (b) The plot of DL-Met Concentration against R_s in 0.05 M HCl solution

It can be concluded from the Nyquist plot that as the concentration of L-Tryp added to the system increased, the R_{ct} and R_s values increased, as illustrated in Figures 7a and 7b. The R_{ct} plot against the L-Tryp concentration is shown in Figure 7a, and the R_s plot against the L-Tryp concentration is shown in Figure 7b.

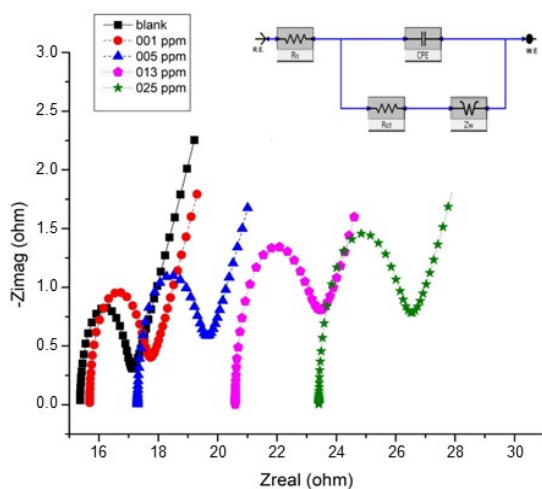


Figure 6. Nyquist plot for carbon steel in 0.05 M HCl with L-Tryp inhibitor

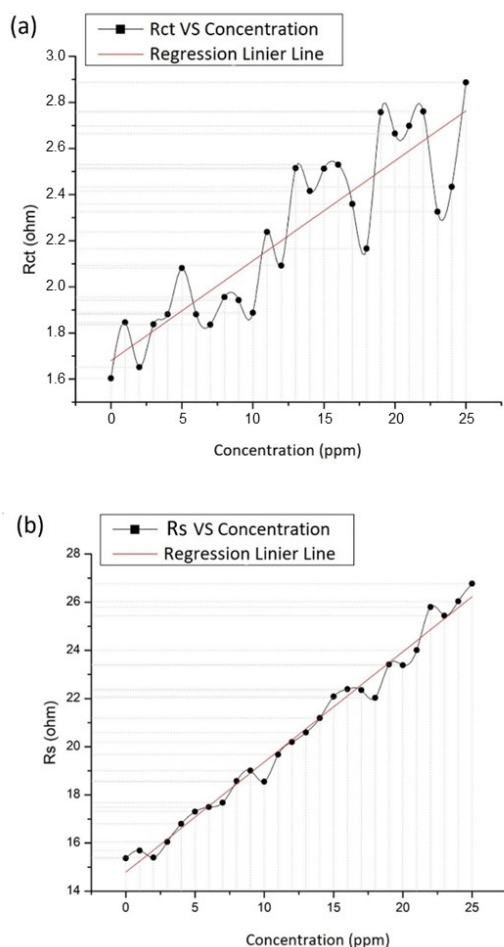


Figure 7. (a) The plot of L-Tryp Concentration against R_{ct} in 0.05 M HCl, and (b) The plot of L-Tryp Concentration against R_s in 0.05 M HCl

Subsequently, using the obtained Nyquist plot, we obtained a Randles equivalent circuit with Warburg. The parameters obtained from this equivalent circuit were used to calculate the inhibition efficiency, and the equivalent circuit parameters for L-Tryp inhibition activity on carbon steel in 0.05 M HCl are shown in Table 4. The highest R_{ct} and R_s values were obtained when the concentration of L-Tryp added to the system was 25 ppm, resulting in a total inhibition efficiency of 87.08%. Therefore, the optimum condition for inhibition activity is at 25 ppm L-Tryp on carbon steel in 0.05 M HCl, and further investigations using the potentiodynamic polarization method are necessary.

Based on the data obtained, this research confirms previous research, which stated that DL-Met and L-Tryp provide inhibitory activity in acidic conditions [28, 30]. In addition, the concentrations of DL-Met and L-Tryp required to inhibit corrosion in conditions approaching a corrosive environment in the oil and gas industry are sufficient to use low concentrations. This is essential information for saving the use of DL-Met and L-Tryp bio-inhibitors in the industrial sector.

EIS measurements were then carried out by measuring the inhibitory activity of DL-Met and L-Tryp at $\text{pH} > 7$ in a 0.05 M NH_4OH solution. Figure 8 shows the Nyquist plot of the EIS measurements of DL-Met inhibition activity on carbon steel in 0.05 M NH_4OH . The Nyquist plot shows that as the concentration of DL-Met increased under alkaline conditions, the R_{ct} and R_s values tended to decrease. Figure 9a shows the R_{ct} plot against DL-Met concentration under alkaline conditions, and Figure 9b shows the R_s plot against DL-Met concentration under alkaline conditions.

Table 3. Parameter data of equivalent circuit components for carbon steel with DL-Met inhibitor in 0.05 M HCl solution

[DL-Met] (ppm)	R_{ct} ($\Omega \text{ cm}^2$)	R_s ($\Omega \text{ cm}^2$)	CPE (mF)	$\eta_{R_{ct}}$ (%)	η_{R_s} (%)	η_{total} (%)
Blank	1.943	17.600	0.212	-	-	-
100	1.863	16.630	4.154	-4.3	-5.8	-10.1
300	2.250	18.980	10.010	13.6	7.23	20.83
525	2.689	22.550	12.780	27.7	22.0	49.7
600	2.530	23.760	14.080	23.2	26.0	49.2

Table 4. Parameter data for equivalent circuit components for carbon steel with L-Tryp inhibitors in 0.05 M HCl solution

[L-Tryp] (ppm)	R_{ct} ($\Omega \text{ cm}^2$)	R_s ($\Omega \text{ cm}^2$)	CPE (mF)	$\eta_{R_{ct}}$ (%)	η_{R_s} (%)	η_{total} (%)
Blank	1.603	15.370	0.429	-	-	-
1	1.846	15.690	1.134	13.160	2.030	15.190
5	2.082	17.300	3.095	23.000	11.150	34.150
13	2.515	20.590	6.216	36.260	25.350	61.610
25	2.887	26.770	6.772	44.500	42.580	87.080

Table 5 shows the equivalent circuit parameter data for carbon steel with the DL-Met inhibitor in a 0.05 M NH₄OH solution. Table 5 shows that the inhibition efficiency became more negative with the addition of DL-Met. Hence, DL-Met's effectiveness as a corrosion inhibitor is limited in alkaline conditions. In fact, under such circumstances, DL-Met not only fails to inhibit corrosion but also accelerates the corrosion rate of carbon steel. This occurs because DL-Met readily dissolves in alkaline conditions, hindering its ability to adsorb onto metal surfaces and forming zwitterions. These zwitterions, in turn, enhance the electrical conductivity of the solution, facilitating the corrosion process.

Furthermore, EIS measurements were carried out to determine the inhibition activity of L-Tryp on carbon steel in a 0.05 M NH₄OH solution. Figure 10 shows the Nyquist plot for measuring L-Tryp inhibition activity on carbon steel in a 0.05 M NH₄OH solution. As L-Tryp was added, the R_{ct} and R_s values decreased. Figure 11a shows the R_{ct} plot against L-Tryp concentration, while Figure 11b shows the R_s plot against L-Tryp concentration.

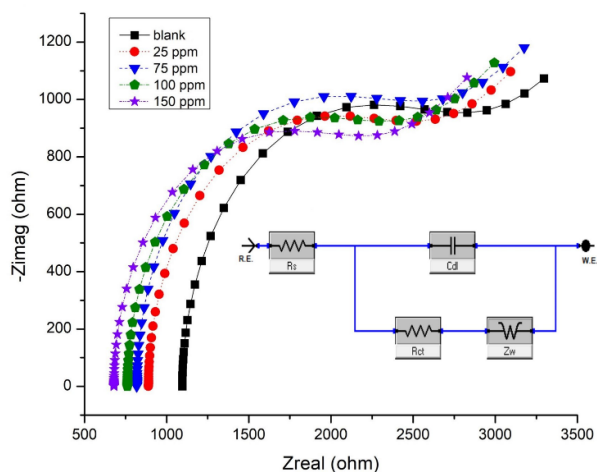


Figure 8. Nyquist plot for carbon steel in 0.05 M NH₄OH with DL-Met inhibitor

Similar to the previous EIS measurements, the Nyquist plot was correlated with the equivalent circuit, leading to the selection of a Randless circuit with the Warburg element as the suitable circuit configuration for this measurement. The R_{ct} parameter can be determined using the equivalent circuit, which will be used to

calculate the inhibition efficiency. Table 6 presents the circuit parameter data for measuring L-Tryp inhibition activity on carbon steel under alkaline conditions. The value of the total inhibition efficiency decreases with the addition of L-Tryp, meaning that L-Tryp cannot be used as an inhibitor for carbon steel in an alkaline state. Therefore, the use of bio-inhibitors DL-Met and L-Tryp is not recommended for industries in corrosive environments caused by alkaline conditions.

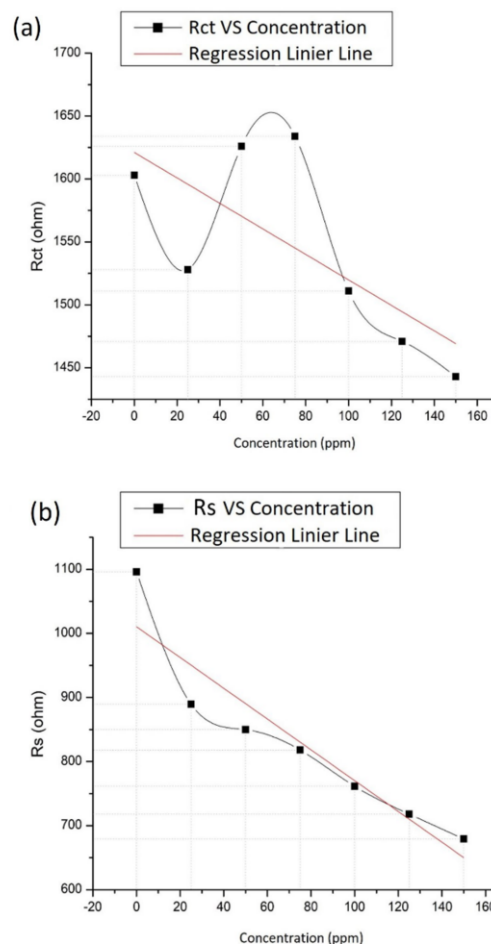


Figure 9. (a) The plot of DL-Met Concentration against R_{ct} in 0.05 M NH₄OH, and (b) The plot of DL-Met Concentration against R_s in 0.05 M NH₄OH

Table 5. Equivalent circuit component parameter data for carbon steel with DL-Met inhibitor in 0.05 M NH₄OH solution

[DL-Met] (ppm)	R _{ct} (Ω cm ²)	R _s (Ω cm ²)	C _{dl} (mF)	η _{Rct} (%)	η _{Rs} (%)	η _{total} (%)
Blank	1603	1096.000	0.084	-	-	-
25	1528	889.500	0.074	-4.910	-23.210	-28.120
75	1634	818.200	0.070	1.890	-33.950	-32.060
100	1511	761.500	0.070	-6.000	-43.920	-49.920
150	1443	679.100	0.069	-11.000	-61.390	-72.390

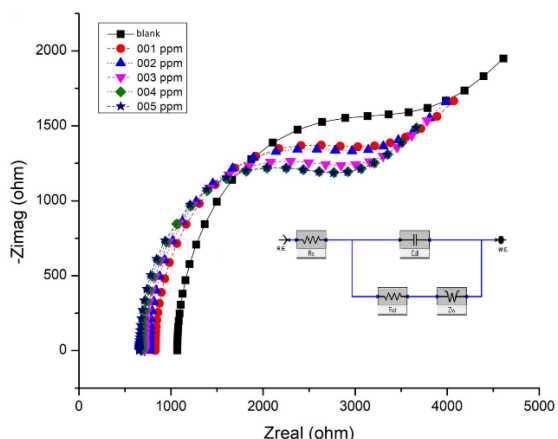


Figure 10. (a) Nyquist plot for carbon steel in 0.05 M NH₄OH with L-Tryp inhibitor

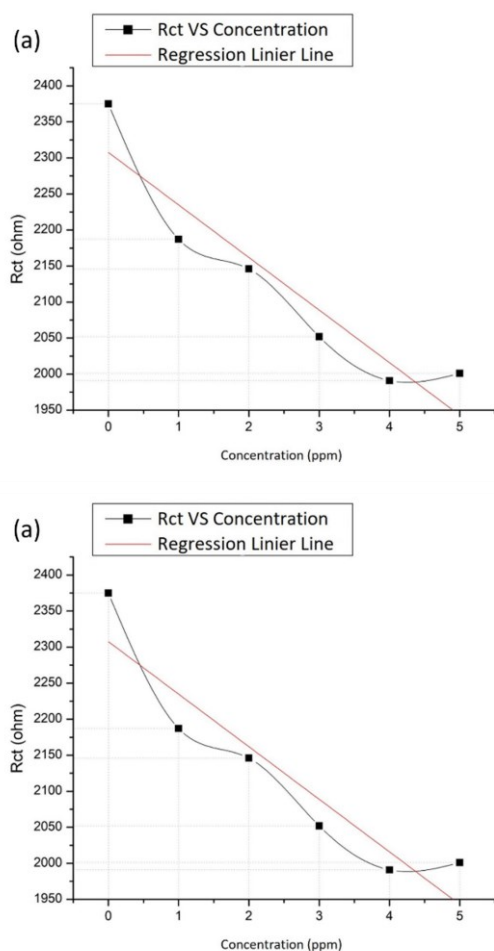


Figure 11. (a) The plot of L-Tryp Concentration against R_{ct} in 0.05 M NH₄OH solution, and (b) The plot of L-Tryp Concentration against R_s in 0.05 M NH₄OH solution

Table 7. Electrochemical Parameters of PDP Measurement for 525 ppm DL-Met inhibitor and 25 ppm L-Tryp inhibitor on carbon steel in 0.05 M HCl solution

Inhibitor	Conc. (ppm)	E _{corr} (mv)	R _p (ohm.cm ²)	i _{corr} (mA/cm ²)	B _a (mV)	B _c (mV)	Corrosion Rate (mm/year)
DL-Met	0	-448.200	34.120	0.857	229.300	-187.800	10.020
	525	-417.700	73.440	0.382	112.000	-157.500	4.468
L-Tryp	0	-448.200	34.120	0.857	229.300	-187.800	10.020
	25	-422.200	68.740	0.427	142.000	-231.200	5.003

Table 6. Parameter data for equivalent circuit components for carbon steel with L-Tryp inhibitors in 0.05 M NH₄OH solution

[L-Tryp] (ppm)	R _{ct} (Ω cm ²)	R _s (Ω cm ²)	C _{dl} (uF)	η R _{ct} (%)	η R _s (%)	η _{total} (%)
Blank	2375	1069.000	0.051	-	-	-
1	2187	830.500	0.050	-8.590	-28.710	-37.300
2	2146	765.300	0.048	-10.670	-39.680	-50.350
3	2052	713.300	0.048	-15.740	-49.860	-65.600
4	1991	677.300	0.047	-19.280	-57.830	-77.110
5	2001	655.000	0.046	-18.690	-63.206	-81.900

3.2. PDP Data Interpretation and Processing

In this study, PDP measurements were conducted to determine the inhibitory activity at optimum pH and concentration conditions. In this case, the optimum conditions are the acidic state, with 525 ppm DL-Met inhibitor and 25 ppm L-Tryp inhibitor having the highest Nyquist curve peak. Electrochemical parameters such as the free corrosion potential E_{corr}, corrosion current strength I_{corr}, resistance R_p, B_a anodic Tafel slope, and B_c cathodic Tafel were determined by measuring the PDP. In addition, the corrosion rate per year was predicted using the PDP method.

Figure 12a shows a Tafel plot for measuring inhibition activity on carbon steel with 525 ppm DL-Met inhibitor in 0.05 M HCl solution. In comparison, Figure 12b shows a Tafel plot for measuring inhibition activity on carbon steel with 25 ppm L-Tryp inhibitor in an HCl solution. Table 7 displays the electrochemical parameter data of PDP measurements for 525 ppm DL-Met inhibitor and 25 ppm L-Tryp inhibitor on carbon steel in a 0.05 M HCl solution. The E_{corr} parameter did not change significantly for DL-Met or L-Tryp inhibitors compared to the blank. Therefore, it can be concluded that these two inhibitors are mixed or support inhibitors.

The i_{corr} PDP measurement value decreased for DL-Met and L-Tryp inhibitors compared to the blank. This indicates that both inhibitors can reduce the corrosion rate of carbon steel under acidic conditions. Furthermore, the R_p value for both inhibitors increased significantly, which means that the inhibitors can form a protective layer on the surface of the carbon steel and inhibit the corrosion process.

The slope of the B_a anode Tafel and B_c cathode Tafel for DL-Met did not change significantly, indicating that the inhibitor did not affect the anodic or cathodic reactions significantly. Nonetheless, the change in B_c is more notable than the change in B_a , indicating that this bio-inhibitor falls into the cathodic bio-inhibitor category. Its operational principle involves functioning as a cation that migrates towards the metal cathode area, and it can inhibit the reduction reaction rate at the cathode, undergoing chemical and electrochemical transformations to form a protective layer that effectively hinders the corrosion process [38].

However, for L-Tryp, the slope of the B_a anode Tafel and B_c cathode Tafel values decreased significantly, indicating that the inhibitor can affect both anodic and cathodic reactions. Hence, L-Tryp can be classified as a mixed-type inhibitor, functioning through the principle of chemical bonding with the metal surface due to the pairing of free electrons from heteroatoms in the mixed inhibitor. Therefore, it can inhibit the reduction reaction rate at the cathode and the oxidation reaction rate at the anode through electron transfer inhibition [39]. This monomolecular layer forms and adheres to the metal surface in both the cathodic and anodic regions, effectively impeding corrosion in both areas.

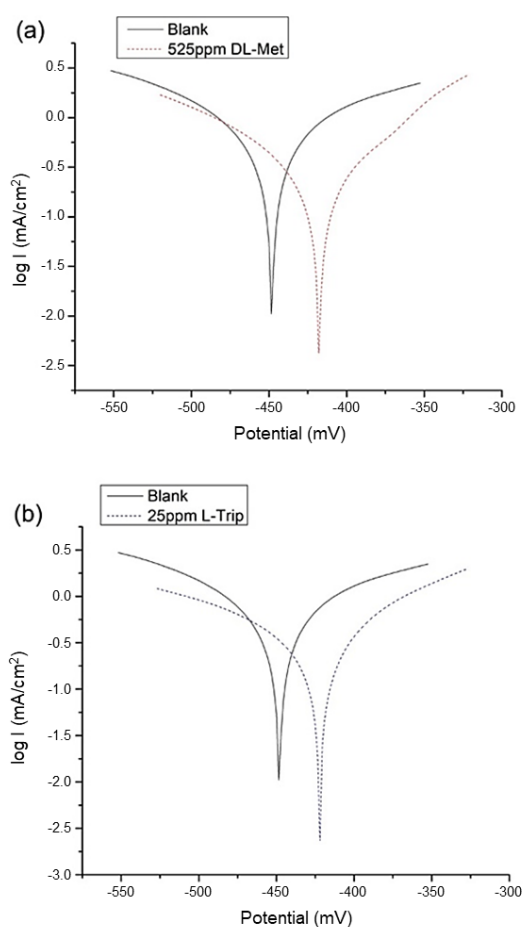


Figure 12. (a) The plot of Tafel 525 ppm DL-Met in 0.05 M HCl, and (b) The plot of Tafel 25 ppm L-Tryp in 0.05 M HCl

3.3. Effect of pH on DL-Tryp and L-Tryp Inhibitory Activities

Based on the investigation, it can be concluded that DL-Met and L-Tryp serve as corrosion inhibitors in acidic settings. This association is closely linked to the structural alterations that occur when DL-Met and L-Tryp undergo protonation within an acidic environment [40]. Figure 13 illustrates the protonated forms of D-Met (13a), L-Met (13b), and L-Tryp (13c).

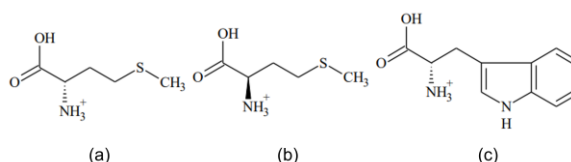


Figure 13. Protonated structures for (a) L-Met, (b) D-Met, and (c) L-Tryp

When the pH is below the pI of an amino acid, it enters the protonated state. DL-Met has a pI of 5.88 [41], and L-Tryp has a pI of 5.74 [27]. Consequently, in a 0.05 M HCl solution, the structures of both DL-Met and L-Tryp are protonated. In this state, both amino acids can still adsorb onto the positively charged carbon steel surface by transferring heteroatom-free electrons (N, O, and S). Furthermore, the presence of π bonds in L-Tryp reinforces its adsorption on carbon steel surfaces. Above the pI value, both amino acids undergo a deprotonated state.

Figure 14 shows the deprotonated states of DL-Met and L-Tryp. At neutral or alkaline pH values, DL-Met and L-Tryp become negatively charged and can attach to the carbon steel surface. However, under these conditions, the metal surface tends to adsorb OH^- from the bulk solution phase more than it adsorbs the amino acids DL-Met and L-Tryp, promoting the corrosion process. As a result, EIS measurements carried out at pH values ≥ 7 revealed a tendency for the R_{ct} and R_s barriers to decrease.

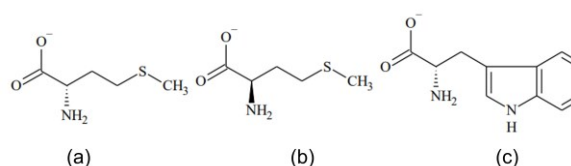


Figure 14. Deprotonated structures for a) L-Met, b) D-Met, and c) L-Tryp

4. Conclusion

In summary, the research findings demonstrate that DL-Met and L-Tryp function as effective inhibitors under acidic conditions, specifically in a 0.05 M HCl solution, as confirmed by Electrochemical Impedance Spectroscopy (EIS) and Potentiodynamic Polarization (PDP) measurements. EIS results show that 525 ppm DL-Met achieves an inhibition efficiency of 49.7%, while 25 ppm L-Tryp exhibits an impressive 87.08% inhibition efficiency. Moreover, the PDP measurements reveal that both DL-Met and L-Tryp act as mixed anodic inhibitors, significantly reducing the corrosion rate from 10.02 mm/year to 4.468 mm/year for 525 ppm DL-Met and to 5.003 mm/year for 25 ppm L-Tryp under acidic

conditions. Furthermore, based on B_a and B_c parameter changes, DL-Met is classified as a cathodic inhibitor, whereas L-Tryp is identified as a mixed inhibitor in acidic environments. It is important to note that DL-Met is not a recommended inhibitor in neutral or alkaline conditions, and similarly, L-Tryp is unsuitable as a corrosion inhibitor in alkaline environments. Consequently, these research findings hold significant implications for selecting DL-Met and L-Tryp bio-inhibitors, particularly in industries with acidic corrosive environments, such as the petroleum industry. This research provides valuable insights into the potential applications of DL-Met and L-Tryp as corrosion inhibitors, specifically in acidic settings. It offers a foundation for their utilization in various industrial sectors, with a particular focus on the petroleum industry.

References

- [1] Sri Handani, Megi Septia Elta, Pengaruh inhibitor ekstrak daun pepaya terhadap korosi baja karbon schedule 40 grade B ERW dalam medium air laut dan air tawar, *Jurnal Riset Kimia*, 5, 2, (2012), 175-175 <https://doi.org/10.25077/jrk.v5i2.219>
- [2] Hala A. El Nagy, ElSayed H. El Tamany, Hana Ashour, Olfat E. El-Azabawy, Elsayed G. Zaki, Shimaa M. Elsaed, Polymeric Ionic Liquids Based on Benzimidazole Derivatives as Corrosion Inhibitors for X-65 Carbon Steel Deterioration in Acidic Aqueous Medium: Hydrogen Evolution and Adsorption Studies, *ACS Omega*, 5, 47, (2020), 30577-30586 <https://doi.org/10.1021/acsomega.0c04505>
- [3] Li Feng, Shengtao Zhang, Yujie Qiang, Shenying Xu, Bochuan Tan, Shijin Chen, The synergistic corrosion inhibition study of different chain lengths ionic liquids as green inhibitors for X70 steel in acidic medium, *Materials Chemistry and Physics*, 215, (2018), 229-241 <https://doi.org/10.1016/j.matchemphys.2018.04.054>
- [4] Ebrahim Kamali Ardakani, Elaheh Kowsari, Ali Ehsani, Seeram Ramakrishna, Performance of all ionic liquids as the eco-friendly and sustainable compounds in inhibiting corrosion in various media: A comprehensive review, *Microchemical Journal*, 165, (2021), 106049 <https://doi.org/10.1016/j.microc.2021.106049>
- [5] Vishal Varshney, Abhishek Verma, Vishnu Kumar, Tej Pratap Singh, A review paper on green corrosion and its inhibitors, *International Journal of Materials Science*, 4, 1, (2023), 27-31
- [6] Megawati Zunita, Deana Wahyuningrum, I. Gede Wenten, Raj Boopathy, Carbon steel corrosion inhibition activity of tofu associated proteins, *Bioresource Technology Reports*, 17, (2022), 100973 <https://doi.org/10.1016/j.biteb.2022.100973>
- [7] M. A. Deyab, Sulfonium-based ionic liquid as an anticorrosive agent for thermal desalination units, *Journal of Molecular Liquids*, 296, (2019), 111742 <https://doi.org/10.1016/j.molliq.2019.111742>
- [8] Abhinay Thakur, Ashish Kumar, Shveta Sharma, Richika Ganjoo, Humira Assad, Computational and experimental studies on the efficiency of *Sonchus olerensis* as green corrosion inhibitor for mild steel in 0.5 M HCl solution, *Materials Today: Proceedings*, 66, (2022), 609-621 <https://doi.org/10.1016/j.matpr.2022.06.479>
- [9] Entian Li, Yingping Li, Songling Liu, Pei Yao, Choline amino acid ionic liquids as green corrosion inhibitors of mild steel in acidic medium, *Colloids and Surfaces A: Physicochemical and Engineering Aspects*, 657, (2023), 130541 <https://doi.org/10.1016/j.colsurfa.2022.130541>
- [10] Entian Li, Songling Liu, Fang Luo, Pei Yao, Amino acid imidazole ionic liquids as green corrosion inhibitors for mild steel in neutral media: Synthesis, electrochemistry, surface analysis and theoretical calculations, *Journal of Electroanalytical Chemistry*, 944, (2023), 117650 <https://doi.org/10.1016/j.jelechem.2023.117650>
- [11] S. Kshama Shetty, A. Nityananda Shetty, Eco-friendly benzimidazolium based ionic liquid as a corrosion inhibitor for aluminum alloy composite in acidic media, *Journal of Molecular Liquids*, 225, (2017), 426-438 <https://doi.org/10.1016/j.molliq.2016.11.037>
- [12] F. El-Hajjaji, E. Ech-Chihbi, N. Rezki, F. Benhiba, M. Taleb, Dheeraj Singh Chauhan, M. A. Quraishi, Electrochemical and theoretical insights on the adsorption and corrosion inhibition of novel pyridinium-derived ionic liquids for mild steel in 1 M HCl, *Journal of Molecular Liquids*, 314, (2020), 113737 <https://doi.org/10.1016/j.molliq.2020.113737>
- [13] Xihua Xu, Ambrish Singh, Zhipeng Sun, K. R. Ansari, Yuanhua Lin, Theoretical, thermodynamic and electrochemical analysis of biotin drug as an impending corrosion inhibitor for mild steel in 15% hydrochloric acid, *Royal Society Open Science*, 4, 12, (2017), 170933 <https://doi.org/10.1098/rsos.170933>
- [14] Megawati Zunita, Yosef Juliyus Kevin, Ionic liquids as corrosion inhibitor: From research and development to commercialization, *Results in Engineering*, 15, (2022), 100562 <https://doi.org/10.1016/j.rineng.2022.100562>
- [15] Muhammad Wasim, Milos B. Djukic, External corrosion of oil and gas pipelines: A review of failure mechanisms and predictive preventions, *Journal of Natural Gas Science and Engineering*, 100, (2022), 104467 <https://doi.org/10.1016/j.jngse.2022.104467>
- [16] Tamires Cristina Costa, Letiane Thomas Hendges, Bruna Temochko, Luciana Prazeres Mazur, Belisa Alcantara Marinho, Silvio Edegar Weschenfelder, Priscilla Lopes Florido, Adriano da Silva, Antônio Augusto Ulson de Souza, Selene M. A. Guelli Ulson de Souza, Evaluation of the technical and environmental feasibility of adsorption process to remove water soluble organics from produced water: A review, *Journal of Petroleum Science and Engineering*, 208, (2022), 109360 <https://doi.org/10.1016/j.petrol.2021.109360>
- [17] B. El Ibrahimy, A. Jmiai, L. Bazzi, S. El Issami, Amino acids and their derivatives as corrosion inhibitors for metals and alloys, *Arabian Journal of Chemistry*, 13, 1, (2020), 740-771 <https://doi.org/10.1016/j.arabjc.2017.07.013>
- [18] H. Ashassi-Sorkhabi, Z. Ghasemi, D. Seifzadeh, The inhibition effect of some amino acids towards the corrosion of aluminum in 1M HCl+1M H₂SO₄ solution, *Applied Surface Science*, 249, 1, (2005), 408-418 <https://doi.org/10.1016/j.apsusc.2004.12.016>

- [19] Abdullah Hasan Jabbar, Suhair Mohammad Husein Kamona, Sarah Kamil Abbood, Talib Kh Hussein, Dahlia N. Al-Saidi, Safaa Mustafa Hameed, Rashid Abdul Kareem Rashid, Hussein Abdullah Abbas, Mustafa M. Kadhim, The effective and sustainable application of a green amino acid-based corrosion inhibitor for Cu metal, *Chemical Physics Impact*, 7, (2023), 100316
<https://doi.org/10.1016/j.chphi.2023.100316>
- [20] Sadegh Pour-Ali, Reza Tavangar, Seyedsina Hejazi, Comprehensive assessment of some L-amino acids as eco-friendly corrosion inhibitors for mild steel in HCl: Insights from experimental and theoretical studies, *Journal of Physics and Chemistry of Solids*, 181, (2023), 111550
<https://doi.org/10.1016/j.jpics.2023.111550>
- [21] Q. H. Zhang, N. Xu, Developing two amino acid derivatives as high-efficient corrosion inhibitors for carbon steel in the CO₂-containing environment, *Industrial Crops and Products*, 201, (2023), 116883
<https://doi.org/10.1016/j.indcrop.2023.116883>
- [22] Abhinay Thakur, Savas Kaya, A. S. Abousalem, Shveta Sharma, Richika Ganjoo, Humira Assad, Ashish Kumar, Computational and experimental studies on the corrosion inhibition performance of an aerial extract of *Cnicus Benedictus* weed on the acidic corrosion of mild steel, *Process Safety and Environmental Protection*, 161, (2022), 801-818
<https://doi.org/10.1016/j.psep.2022.03.082>
- [23] Everton de Britto Policarpi, Almir Spinelli, Application of *Hymenaea stigonocarpa* fruit shell extract as eco-friendly corrosion inhibitor for steel in sulfuric acid, *Journal of the Taiwan Institute of Chemical Engineers*, 116, (2020), 215-222
<https://doi.org/10.1016/j.jtice.2020.10.024>
- [24] B. Arifa Farzana, A. Mushira Banu, K. Riaz Ahamed, *Andrographis echinoides* leaves extract as an eco-friendly corrosion inhibitor for mild steel in acid medium, *Materials Today: Proceedings*, 47, (2021), 2080-2090
<https://doi.org/10.1016/j.matpr.2021.04.478>
- [25] Rajesh Haldhar, Dwarika Prasad, Indra Bahadur, Omar Dagdag, Avni Berisha, Evaluation of *Gloriosa superba* seeds extract as corrosion inhibition for low carbon steel in sulfuric acidic medium: A combined experimental and computational studies, *Journal of Molecular Liquids*, 323, (2021), 114958
<https://doi.org/10.1016/j.molliq.2020.114958>
- [26] Q. H. Zhang, Y. Y. Li, Y. Lei, X. Wang, H. F. Liu, G. A. Zhang, Comparison of the synergistic inhibition mechanism of two eco-friendly amino acids combined corrosion inhibitors for carbon steel pipelines in oil and gas production, *Applied Surface Science*, 583, (2022), 152559
<https://doi.org/10.1016/j.apsusc.2022.152559>
- [27] Jia-Jun Fu, Su-Ning Li, Lin-Hua Cao, Ying Wang, Lian-He Yan, Lu-De Lu, L-Tryptophan as green corrosion inhibitor for low carbon steel in hydrochloric acid solution, *Journal of Materials Science*, 45, (2010), 979-986
<https://doi.org/10.1007/s10853-009-4028-0>
- [28] Jiaxin Luo, Xiong Cheng, Chaofa Zhong, Xinhua Chen, Y. W. Ye, H. Zhao, H. Chen, Effect of reaction parameters on the corrosion inhibition behavior of N-doped carbon dots for metal in 1 M HCl solution, *Journal of Molecular Liquids*, 338, (2021), 116783
<https://doi.org/10.1016/j.molliq.2021.116783>
- [29] N. Wint, J. H. Sullivan, D. J. Penney, The Role of pH on the Inhibition of Aqueous Zinc Corrosion by L-tryptophan, *Journal of The Electrochemical Society*, 164, 7, (2017), C356
<https://doi.org/10.1149/2.0981707jes>
- [30] Zhe Zhang, Ningchen Tian, Lingzhi Zhang, Ling Wu, Inhibition of the corrosion of carbon steel in HCl solution by methionine and its derivatives, *Corrosion Science*, 98, (2015), 438-449
<https://doi.org/10.1016/j.corsci.2015.05.048>
- [31] Güray Kılınççeker, Hasan Demir, The inhibition effects of methionine on corrosion behavior of copper in 3.5% NaCl solution at pH = 8.5, *Protection of Metals and Physical Chemistry of Surfaces*, 49, (2013), 788-797
<https://doi.org/10.1134/S2070205113060221>
- [32] Dong-Ying Li, Yi-Chin Cho, Ming Huang Hsu, Yi-Pin Lin, Recovery of phosphate and ammonia from wastewater via struvite precipitation using spent refractory brick gravel from steel industry, *Journal of Environmental Management*, 302, (2022), 114110
<https://doi.org/10.1016/j.jenvman.2021.114110>
- [33] L. P. Gossen, L. M. Velichkina, Environmental problems of the oil-and-gas industry (Review), *Petroleum Chemistry*, 46, (2006), 67-72
<https://doi.org/10.1134/S0965544106020010>
- [34] Uwe Reimer, Yun Cai, Ruiyu Li, Dieter Froning, Werner Lehnert, Time Dependence of the Open Circuit Potential of Platinum Disk Electrodes in Half Cell Experiments, *Journal of The Electrochemical Society*, 166, 7, (2019), F3098
<https://doi.org/10.1149/2.0121907jes>
- [35] Mohammed Aider, Djamel Djenane, Wassef B. Ounis, Amino acid composition, foaming, emulsifying properties and surface hydrophobicity of mustard protein isolate as affected by pH and NaCl, *International Journal of Food Science & Technology*, 47, 5, (2012), 1028-1036
<https://doi.org/10.1111/j.1365-2621.2012.02937.x>
- [36] Hamad M. Adress Hasan, Ibrahim H. Habib, Ahlam M. Ali, Spectrophotometric Determination of The Ionization Constants of Methionine, Cystine and Cysteine, *European Chemical Bulletin*, 6, 8, (2017), 355-358
- [37] Patrick S. Germain, Wendy G. Pell, Brian E. Conway, Evaluation and origins of the difference between double-layer capacitance behaviour at Au-metal and oxidized Au surfaces, *Electrochimica Acta*, 49, 11, (2004), 1775-1788
<https://doi.org/10.1016/j.electacta.2003.12.009>
- [38] A. Kadhim, A. A. Al-Amiery, R. Alazawi, M. K. S. Al-Ghezi, R. H. Abass, Corrosion inhibitors. A review, *International Journal of Corrosion and Scale Inhibition*, 10, 1, (2021), 54-67
<http://dx.doi.org/10.17675/2305-6894-2021-10-1-3>
- [39] F. El-Hajjaji, E. Ech-chihbi, N. Rezki, F. Benhiba, M. Taleb, Dheeraj Singh Chauhan, M. A. Quraishi, Electrochemical and theoretical insights on the adsorption and corrosion inhibition of novel pyridinium-derived ionic liquids for mild steel in 1 M HCl, *Journal of Molecular Liquids*, 314, (2020), 113737
<https://doi.org/10.1016/j.molliq.2020.113737>

- [40] Husnul Fuad Zein, Ibrar Alam, Piyapong Asanithi, Thana Sutthibutpong, Molecular dynamics study on the effects of charged amino acid distribution under low pH condition to the unfolding of hen egg white lysozyme and formation of beta strands, *PLoS One*, 17, 3, (2022), e0249742
<https://doi.org/10.1371/journal.pone.0249742>
- [41] Chunzheng Li, Gang Gui, Li Zhang, Anqi Qin, Chen Zhou, Xiaoming Zha, Overview of Methionine Adenosyltransferase 2A (MAT2A) as an Anticancer Target: Structure, Function, and Inhibitors, *Journal of Medicinal Chemistry*, 65, 14, (2022), 9531-9547
<https://doi.org/10.1021/acs.jmedchem.2c00395>